Time-resolved experiments in the frequency domain using synchrotron radiation (invited)

Gelsomina De Stasio
Istituto di Struttura della Materia del Consiglio Nazionale delle Ricerche, Via Enrico Fermi, 38, 00044, Frascati, Rome, Italy

A. M. Giusti, T. Parasassi, and G. Ravagnan
Istituto di Medicina Sperimentale del Consiglio Nazionale delle Ricerche, Viale Marx, 15, 00137, Rome, Italy

O. Sapora
Laboratorio di Tossicologia Comparata ed Ecotossicologia, Istituto Superiore di Sanita', Viale Regina Elena, 279, 00161, Rome, Italy

(Presented on 18 July 1991)

PLASTIQUE is the only synchrotron radiation beam line in the world that performs time-resolved fluorescence experiments in frequency domain. These experiments are extremely valuable sources of information on the structure and the dynamics of molecules. This technique measures fluorescence lifetimes with picosecond resolution in the near UV spectral range. Such accurate measurements are rendered possible by taking phase and modulation data, and by the advantages of the cross-correlation technique. A successful experiment demonstrated the radiation damage induced by low doses of radiation on rabbit blood cell membranes.

I. INTRODUCTION

Time-resolved fluorescence is one of the leading techniques in molecular dynamics. Only in recent years, however, this technique has exploited the unique characteristics of synchrotron radiation (SR). We describe PLASTIQUE, the only operating synchrotron radiation beam line for frequency-domain fluorometry.[1] In particular, PLASTIQUE is the only fluorescence facility of its kind for near UV photons, with a total range of 200–800 nm (Fig. 1). No tunable conventional sources exist for the lower part of this spectrum.

II. A BEAMLINE FOR FLUORESCENCE

A pulsed light source as provided by synchrotron radiation is uniquely suited for excitation in time-resolved fluorescence, because of the possibility of continuously varying the wavelength range, and because of the short duration and high repetition rate of the pulse. Generally, the fluorescence emission after pulse excitation is measured in the time domain, using the popular technique of the time-correlated single-photon counting (SPC). Phase fluorometry, however, can also be used in conjunction with a high repetition rate pulsed light source, with the advantages of the armonic method. These advantages include the high accuracy of the lifetime determination, the ease of measuring subnanosecond lifetimes, and the rapidity of data collection.[2]

Ordinarily, multifrequency phase fluorometry is implemented with sinusoidally modulated sources.[2] The time structure of synchrotron radiation simultaneously provides a large number of modulation frequencies. PLASTIQUE is connected to the storage ring Adone at the Frascati National Laboratory, whose single-bunch Gaussian light pulse contains a set of harmonic frequencies 2.856 167 MHz apart ("comb function"), with a Gaussian envelope half-width of 500 MHz.[3] A pioneering work by Weber *et al.* made it possible to extract a single harmonic frequency with a powerful technique: the cross-correlation method.[4]

The wide emission spectrum of synchrotron radiation provides a tunable excitation light source. This opens the way to direct differential measurements of fluorescence excitated by different wavelengths. With PLASTIQUE, these measurements are implemented in a wide range, 200–800 nm; neither tunable lasers nor lamps exist in the 200–260-nm portion of the range. PLASTIQUE is used by a wide variety of users from Italy and the U.S., for experiments in diverse areas of the life sciences and materials science.

III. TECHNICAL DESCRIPTION

PLASTIQUE collects synchrotron radiation emitted by a bending magnet on the 1.5-GeV storage ring Adone,

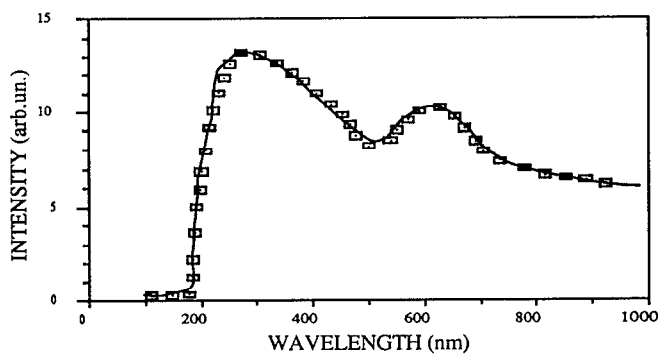

FIG. 1. The intensity spectrum of PLASTIQUE. The low wavelength limit is determined by the cutoff of the fused silica window.

 0034-6748/92/011393-06$02.00

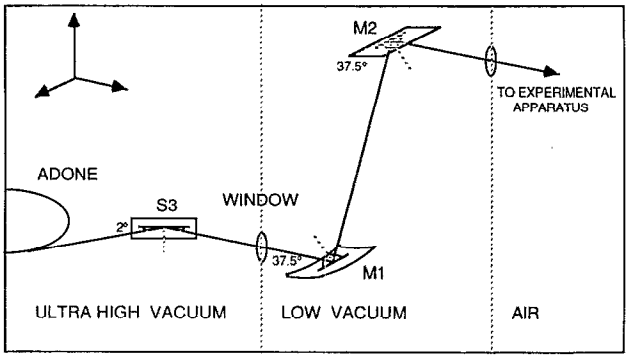

FIG. 2. The layout of PLASTIQUE on the Adone storage ring. Note the three sections: ultra-high vacuum; low vacuum; and air pressure.

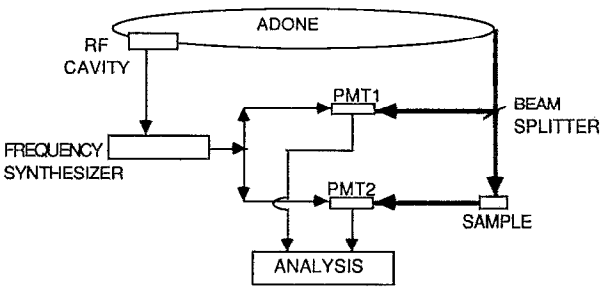

FIG. 3. The block diagram of the multifrequency phase and modulation fluorometer.

over 2.5 mrad on the horizontal plane, and 4 mrad on the vertical plane. Figure 2 shows an overall view of the beam line. The radiation is deflected and separated from the x-ray beam of an adjacent beam line by means of a 2° incidence plane mirror (S3 in Fig. 2) at 11 m from the source. A fused silica window separates the ultrahigh vacuum ($p = 10^{-9}$ mbar) section connected to the storage ring from the low vacuum ($p = 10^{-3}$ mbar) beam line.

A spherical focusing mirror (M1), with a 25.0-m curvature radius, deflects the beam upward by a 105° angle. Another plane mirror (M2) restores the horizontal direction. All the three mirrors, S3, M1, and M2, are aluminum and magnesium fluoride coated. A second fused silica window separates the low vacuum chamber from the atmosphere. After this window, therefore, the beam travels in air. The light is focused by a cylindrical silica lens to the entrance slit of the monochromator, followed by the experimental apparatus.

We do not need ultrahigh vacuum, because light in our spectral range does not interfere significantly with air, and a low vacuum is sufficient to maintain the mirror surfaces clean. The high-energy cutoff is determined by the insertion of silica windows (7.75 eV). The low vacuum section is completely built using PVC pipes, inspirating the name of the beam line. Vacuum tests were made on several kinds of plastics. Low and high density polyethylene did not show enough mechanical stiffness. Polycarbonate was mechanically adequate, but large pipes were not readily available (we needed a diameter >70 mm). Polyvinylchloride (PVC) was chosen because it satisfies all mechanical requirements, and it is capable of maintaining a 10^{-3} mbar pressure. Furthermore, PVC is particularly simple to machine and very light, making it easy to sustain the vacuum pipe from the laboratory's ceiling.

IV. EXPERIMENTAL TECHNIQUE

A spherical grating monochromator (Jobin-Yvon H10 equipped with 1200-lines/mm grating, focal length 10 cm, $f = 3.5$) sends the beam to an optical module KOALA ISS, Inc., Champaign, IL) equipped with a rotating turret to permit easy exchange between sample and reference. This turret is moved by a synchronous motor. Liquids in standard fluorescence cuvettes as well as solid samples can be analyzed. For liquid samples, a circulating thermostatic bath can be used to control the temperature, and a magnetic stirrer to stir the samples during measurements. The sample emission is collected by a large aperture lens and focused onto a photomultiplier PMT2 (Hamamatsu R926). A quartz beam splitter is placed in the optical path before the sample, to direct a fraction of the exciting light to a reference photomultiplier (PMT1), that measures the intensity and phase of the excitation signal (Fig. 3).

A slave frequency synthesizer (Marconi Instruments 10-kHz–1-GHz signal generator 2022A) is in phase with the synthesizer that drives the rf cavity of the storage ring, thus with the light pulse repetition frequency.

Note that the *slave* frequency synthesizer takes, a reference signal, the output of the synthesizer that drives the rf cavity. This output is extremely stable and reproducible, about one order of magnitude better than the synthesizers usually used on conventional phase fluorometers, or in the first synchrotron radiation fluorometer built in Frascati in 1983.[3] It results in ten times more accurate phase measurements, or in ten times shorter acquisition time.

The output of the slave synthesizer can be varied in order to obtain a frequency equal to Adone's fundamental, or to one of the harmonic components, plus 40 Hz. The small difference, 40 Hz, is the cross-correlation frequency. The output of the synthesizer is amplified by an rf power amplifier (ENI 503L), split in two equal parts and applied to the second dynode of the PMTs to implement the cross-correlation technique. We can now perform experiments up to about 330 MHz, even if in principle it is possible to push data acquisition up to the limits of the frequency synthesizer (1 GHz). The actual limit is imposed by the photomultipliers maximum operational frequency.

The outputs of the two PMTs are analyzed separately by two identical channels (CH1 and CH2) in the analysis unit (ISS GREG 80). The two signals are amplified and separated into dc and ac components. The dc component is integrated, to generate a dc signal proportional to the average intensity of the detected signal. The ac component is sent to an amplifier and filtered by a bandpass active filter to select the 40-Hz component. The output of the filter is rectified and integrated to produce a continuous voltage proportional to the ac component. The dc and ac parts of each channel are continuously monitored by four digital

voltmeters, not used for data acquisition, but only for rapid inspection of the signal levels. Accurate measurements of the signals are performed by a precision 13 bits integrating digital voltmeter with 0.1-mV resolution.

The output of the electronics described before is interfaced with an IBM PS 30 computer, that for each frequency calculates the demodulation ratio M:

$$M = (ac_{em}/dc_{em})/(ac_{ex}/dc_{ex}). \quad (1)$$

The phase difference between the reference and the sample signal ϕ is measured by a digital phasemeter. The output of two active filters (CH1 and 2) are sent to zero-crossing detectors, where two square waves are produced. The positive square waves are used to start and stop the phase counter in the computer interface. The resolution for phase measurements is 1 μs, which corresponds to an angular resolution of about 0.01°.

From the two simple equations

$$\phi = \tan \omega\tau_\phi \quad (2)$$

and

$$M = (1 + \omega^2\tau_M^2)^{-1/2} \quad (3)$$

we can calculate the phase and modulation lifetimes τ_ϕ and τ_M.

V. A SUCCESSFUL EXPERIMENT ON THE ALTERATIONS IN ERYTHROCYTE MEMBRANE LIPIDS INDUCED BY LOW DOSES OF IONIZING RADIATION

More than 20 years ago Alper *et al.* proposed membrane lipid damage plays a key role cell killing by ionizing radiation.[5] Such a role is still an open question, despite the large number of experiments that have been used to assess it. Moreover, there have been no successful methods to detect membrane lipid damage induced by low doses of ionizing radiation or the eventual contribution of this damage to mammalian cell death.[6,7]

Studies on the loss of membrane functional properties induced by ionizing radiation have been performed on a variety of biological samples using different methods.[8–12] However, the detection of initial damage required radiation doses higher than those used for cell survival measurements, or the damage was not dose dependent, or required hours and, in some cases, days after irradiation to be observable.[13–15] Spectroscopic techniques such as electron spin resonance, nuclear magnetic resonance, and differential phase fluorometry have been used to detect membrane lipid modification by ionizing radiation.[16–18] The doses used were greater by at least an order of magnitude with respect to the doses used to measure cell survival. For instance, electron spin resonance (ESR) experiments detect modifications after doses > 100 Gy, while the survival of most of the studied cells is already reduced to 1% after a dose of 10 Gy.

The search for a sensitive technique to detect the production of damage and the identification of its molecular nature can be of relevance in the definition of membrane lipids as targets for ionizing radiation, and in the understanding of the biological meaning of such a damage.

We propose multifrequency phase fluorometry as a valuable tool to quantitatively detect membrane damage, particularly after *low* doses of ionizing radiation, and to understand the biological significance of the radiation-induced variations.

In the present study we used the fluorescence lifetime of 1,6-diphenyl-1,3,5-hexatriene (DPH) (Molecular Probes Inc., OR) to monitor the variation of membrane properties in rabbit erythrocyte ghosts irradiated both in the dose range used for cell survival studies and well above. DPH is a hydrophobic molecule, located along the fatty acyl chains of the phospholipid bilayer that forms the cell membrane.[19] Its fluorescence decay in synthetic and cellular membranes can be satisfactorily described by a continuous distribution of lifetime values.[20,21] The DPH heterogeneous decay reflects the heterogeneity of the physical properties of its environment, its lifetime value being inversely related to the dielectric constant of the medium.[22] The width of the DPH lifetime distribution is very sensitive to changes in the composition and dynamics of cell membranes and can be used to investigate physiological and pathological events.[21,23,24]

VI. FLUORESCENCE MEASUREMENTS

Samples of 1 ml (1.8-mg protein/ml) were irradiated with a Siemens Stabilipan x-ray apparatus operating at 200 kV, 15 mA, and with a 0.2-mm Cu filter, at a dose rate ranging between 1 and 20 Gy/min. For the experiments performed in the absence of oxygen, 1 ml of the ghosts' suspension was placed in a glass vial capped with a silicone rubber gasket through which input and output needles were inserted. The ghosts' suspension was degassed with a mixture of 95% N_2 and 5% CO_2 for about 20 min and then the vial was sealed and immediately irradiated. We irradiated the ghosts and not the erythrocytes, since the lysis was not effective on irradiated intact erythrocytes, as judged by the permanence of hemoglobin residues after repeated washing cycles. Hemoglobin acts as a quencher of DPH fluorescence.

Lifetime measurements were performed with 357-nm excitation wavelength and a 16-nm bandwidth. Emission was observed through a 420-nm cut-off filter (Andover Co., NH). The fluorescence background of unlabeled ghosts was $< 0.5\%$ of the total fluorescence.

For lifetime experiments, a solution of 2-2′-*p*-phenylenebis (5-phenyl) oxazole (POPOP) in ethanol was used as reference solution (lifetime 1.35 ns). Phase and modulation data were collected for 9 to 11 modulation frequencies, in the range from 2 to 80 MHz. In all the experiments the sample cell holder was kept at 20 °C. Data were analyzed using the Globals Unlimited software from the Laboratory for Fluorescence Dynamics (University of Illinois at Urbana-Champaign).[25] The goodness of fit was evaluated by the value of the reduced chi-square. Chi-square minimization was performed using a simplex algorithm.[26] The lifetimes fitting function was the sum of two continuously distributed Lorentzian components. The two distributions

TABLE I. DPH lifetime distribution parameters in erythrocyte ghosts, irradiated in the presence or in the absence of oxygen, with different radiation doses.[a]

Gy	$C1$	$W1$	$f1$	$C2$	$W2$	$f2$	Chi-square
0	10.60	2.21±0.07	0.93	0.98	0.21	0.07	3.79
In the presence of oxygen							
0.5	9.94	1.73	0.94	0.08	0.12	0.06	2.82
1.2	10.33	1.66	0.98	0.08	0.18	0.02	2.72
2.5	10.70	1.37	0.97	0.07	0.18	0.03	2.51
5.0	10.53	1.21	0.98	0.12	0.15	0.02	5.34
7.5	10.64	1.08	0.99	0.17	0.17	0.01	4.42
12.0	10.76	0.93	0.91	0.09	0.20	0.09	2.48
22.0	10.50	0.76±0.02	0.93	0.13	0.22	0.07	3.39
44.0	10.30	0.70	0.97	0.18	0.17	0.03	9.82
88.0	10.62	0.61	0.98	0.21	0.19	0.02	2.69
110.0	10.26	0.53	0.92	0.61	0.59	0.08	1.81
220.0	10.98	0.48	0.92	1.37	1.18	0.08	2.20
330.0	11.54	0.39	0.81	3.35	4.94	0.19	1.24
440.0	10.20	0.12	0.69	4.49	5.33	0.31	0.32
550.0	11.96	0.06	0.55	6.74	6.38	0.45	2.79
In the absence of oxygen							
5.0	10.48	2.01	0.93	0.20	0.20	0.07	2.84
12.0	10.40	2.21	0.96	0.20	0.19	0.04	3.38
22.0	10.54	2.04	0.93	0.19	0.20	0.07	1.92
44.0	10.51	2.16	0.93	0.20	0.20	0.07	2.41
220.0	11.27	2.08	0.93	0.20	0.20	0.07	4.88
330.0	10.33	2.29	0.98	0.26	0.09	0.02	2.97
550.0	10.64	2.03	0.98	0.11	0.06	0.02	1.32

[a]Values of the center, full width at half-maximum and fractional intensity of the long ($C1$, $W1$, and $f1$, respectively) and short ($C2$, $W2$, and $f2$) lifetime components of the decay. For the width values of 0- and 22-Gy experiments the standard deviations have been calculated as described in the text.

were characterized by three parameters each: the center, the full width at half-maximum (FWHM), and the fractional intensity.

The experimental errors in the resulting parameters were evaluated as the standard deviation of each parameter over two sets of 10 different samples, unirradiated and irradiated with 22 Gy, respectively. To account for the biological variability, for the different preparations of ghosts and for the stability of samples, each set included samples: (i) from the same rabbit with different preparations; (ii) from different rabbits with simultaneous preparations; and (iii) from the same rabbit with simultaneous preparation but labeled and measured after 24-h storage at 0–4 °C. The results were used to evaluate the standard deviations reported in Table I for the two conditions.

VII. RESULTS

The effect of ionizing radiation on rabbit erythrocyte ghosts was followed by measuring the width of the fluorescence lifetime distribution of DPH. The DPH fluorescence decay in unirradiated erythrocyte ghosts was characterized by a main distributed component with the fractional intensity of about 95% and a center value of about 10.5 ns (Fig. 4). The width of the main component was about 2.2 ns. A second short-lived component was also present, with a fractional intensity of about 5%, centered at about 0.1 ns and with a distribution width of about 0.2 ns.

Figure 4 shows the fluorescence lifetime distribution of DPH in erythrocyte ghosts after different doses of radiation. In irradiated samples, in the low dose range, the width value of the main component showed a decrease as a function of the dose, while the center value was constant. In the high dose range, 220 and 440 Gy, an increase in the fractional intensity of the short lifetime component of the

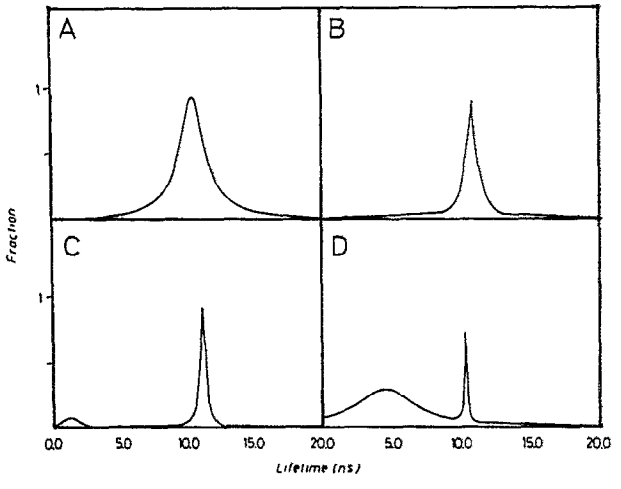

FIG. 4. DPH continuous lifetime distribution in rabbit erythrocyte ghosts: unirradiated (a); irradiated in air with a dose of 12 (b); 220 (c); and 440 Gy (d). Measurements at 20 °C.

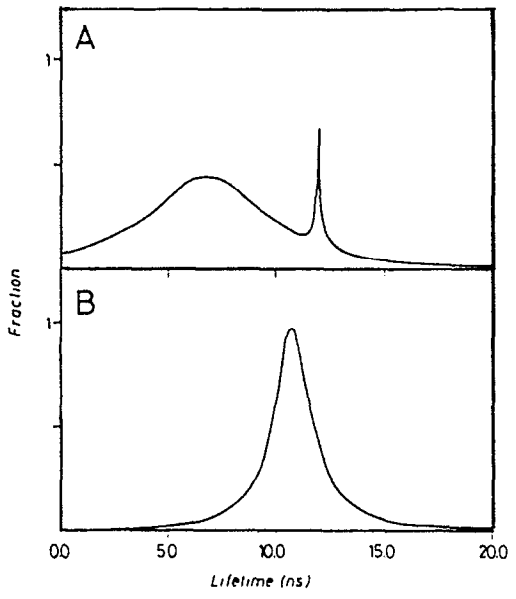

FIG. 5. DPH continuous lifetime distribution in rabbit erythrocyte ghosts: unirradiated (a); irradiated with a dose of 550 Gy in the presence (a) and in the absence (b) of oxygen.

decay was observed. When the irradiation was performed under anoxic conditions neither variations in the fractional intensity nor in the distribution width of both components of DPH decay were observed (Fig. 5).

Figure 6 shows the decrease in the width of the distribution of the main component of DPH decay as a function of the logarithm of radiation dose. After a dose of 12 Gy the width of the DPH lifetime distribution decreases more than a factor of 2 with respect to unirradiated ghosts. The width decrease was a linear function of the logarithm of the dose. No appreciable variations were observed in the center

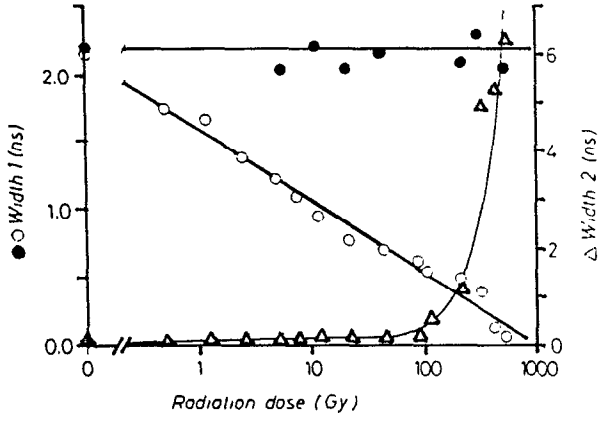

FIG. 6. Values of the full width at half-maximum (width) of the long (○,●) and short (△) lifetime components of DPH decay in rabbit erythrocyte ghosts as a function of the radiation dose. Irradiation performed in the presence (○,△) or in the absence (●) of oxygen. Measurements at 20 °C.

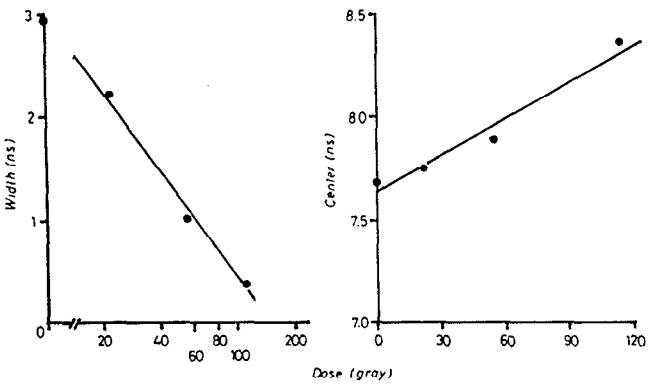

FIG. 7. Effect of radiation on the distribution of DPH main lifetime component in multilamellar DOPC liposomes, as a function of the dose. Values of the full width at half-maximum (width) and of the distribution center.

values of the distribution (about 10.5 ns). In Fig. 6 the width of the long lifetime component in erythrocyte ghosts irradiated in the absence of oxygen is also reported. The width values were constant at all doses. The short component of DPH decay was not affected by doses of radiation up to 110 Gy, while at higher doses its width increases progressively (Fig. 6).

Multilamellar DOPC and DPPC liposomes were irradiated in the dose range from 22 to 110 Gy. No variation of the DPH lifetime distribution was observed in irradiated DPPC samples. In Fig. 7 the results obtained using DOPC-irradiated vesicles are reported. The width of DPH lifetime distribution decreased linearly with the logarithm of the dose, while the center of the distribution increased linearly with the dose.

VIII. DISCUSSION

We report the first observation of large variations of structure and dynamics of membrane lipids induced by ionizing radiation in the low-dose range. Although our biological samples are a simplified system, we believe it to be a representative model of cell membranes.

In the present study we have measured the DPH lifetime distribution in erythrocyte ghosts using multifrequency phase and modulation fluorometry. The technique is particularly suited for the resolution of heterogeneous, multicomponent, fluorescence decays. Generally, the intrinsic and extrinsic fluorescence arising from biological samples is characterized by a multicomponent decay, reflecting the heterogeneity of the natural material. Among several molecules used to fluorescently label the hydrophobic core of lipid bilayers, DPH is one of the more popular and better characterized.[19,22] The heterogeneity of its decay in membranes has been best described by two distributed components having Lorentzian shape. In synthetic and natural membranes the values of the center and the width of the distribution of the main component have been found to depend on the composition and the phase state of the membrane lipids.[20,21] In particular, since the DPH lifetime value is inversely related to the dielectric constant of the

environment, and since a gradient of water concentration exists along the bilayer depth, the width value of the DPH lifetime is considered to reflect the heterogeneous water concentration in the hydrophobic core of the bilayer. Changes in the width values observed during cell physiological processes have been attributed to the variation of water concentration in the bilayer core, due to different dynamics and composition of the lipids.[21,23,24] The short-lived component of the DPH decay originates from photophysical properties of the probe and its fractional intensity can be increased by heavy photodecomposition of the system.[22,26] By measuring DPH decay in erythrocyte ghosts as a function of dose in the low-dose range, we observed a dose-dependent decrease of the width of the distribution of the main component of the decay. In our experimental conditions the width decrease is observable at a lower limit of 0.5 Gy. We believe that the observed variations are due to the formation of oxidation products in the membrane lipids. Actually, measurements performed in oxygen-free conditions did not show any variation in the width of the DPH lifetime distribution.

According to Konings, oxidation processes of unsaturated lipid produce chain reactions, locally amplifying the initial damage, leading to the formation of hydroperoxides and acyl-chain crosslinkages.[7] Nevertheless, using spectroscopic and biochemical techniques the detection and quantitation of lipid oxidation products in membranes required high radiation doses.[27,28]

The attribution of a molecular origin to the observed width variation of the DPH fluorescence lifetime distribution in erythrocyte ghosts requires further studies. As a possible hypothesis, the production of hydroperoxides and crosslinkages in the membrane lipids can disorder the upper region of the bilayer, favoring the penetration of water. The presence of water will quench the fluorescence of those DPH molecules close to the bilayer surface. The residual fluorescence will then originate from DPH molecules located in the inner hydrophobic region of the bilayer. The resulting width value of the DPH lifetime distribution is expected to be lower, due to the relative homogeneity of this hydrophobic environment, and the value of the center will increase due to the low polarity. This hypothesis is consistent with the increase of the polarization value, a parameter sensitive to the order of the system.[18] With this hypothesis in mind, we performed experiments in multilamellar DOPC and DPPC liposomes, irradiated with different doses. In the unsaturated DOPC liposomes the width of the main component of DPH decay decreases linearly with the logarithm of radiation dose and the value of the center increases linearly with the radiation dose (Fig. 7).

No effects of ionizing radiation is observed in saturated DPPC liposomes.

The DPH decay is also characterized by a small fraction of a short-lifetime component, sensitive to the presence of lipid decomposition products.[26] The pronounced increase of the fractional intensity of this component observed after irradiation of erythrocyte ghosts in the high-dose range must be considered indicative of severe membrane damage. The molecular nature of such damage cannot be assessed at the moment. This is likely to be damage detected by other spectroscopic techniques after irradiation of erythrocyte ghosts in the high-dose range.[16,17]

In conclusion, we present experimental evidence of alterations on cell membrane lipids in the same dose range used for cell survival studies, and for the detection of DNA damage. Since the observed damage strictly depends on the presence of oxygen, there is also good indication that the modification of membrane properties are mainly due to the formation of lipid oxidation products. Using doses higher than 110 Gy, profound damage is caused to lipids. Further studies are needed to elucidate the molecular basis of the low- and high-dose membrane damage, and the role of such damage in cell killing.

[1] F. Antonangeli, G. De Stasio, T. Parasassi, N. Rosato, A. Savoia, and N. Zema, LNF Internal Report 91/006 (IR); G. De Stasio, N. Zema, F. Antonangeli, A. Savoia, T. Parasassi, and N. Rosato, Rev. Sci. Instrum. **62**, 1670 (1991).
[2] E. Gratton and R. Lopez-Delgado, Nuovo Cimento B **56**, 110 (1980).
[3] E. Gratton, D. M. Jameson, N. Rosato, and G. Weber, Rev. Sci. Instrum. **55**, 486 (1984).
[4] R. D. Spencer and G. Weber, Ann. N. Y. Acad. Sci. **158**, 361 (1969).
[5] T. Alper, Nature **217**, 862 (1968); Adv. Exp. Med. Biol. **84**, 1349 (1977).
[6] H. Wolters and A. W. T. Konings, Int. J. Rad. Biol. **46**, 161 (1984).
[7] A. W. T. Konings, *Liposomes Technology*, edited by Gregoriadis (CRC, New York, 1985), Vol. 1.
[8] D. Palecz and W. Leiko, Int. J. Rad. Biol. **44**, 293 (1983).
[9] J. C. Edwards, D. Chapman, W. A. Cramp, and M. B. Yatvin, Progr. Biophys. Mol. Biol. **43**, 71 (1984).
[10] A. C. C. Ruifrok, B. Kanon, and A. W. T. Konings, Radiat. Res. **101**, 326 (1985).
[11] M. J. Mullin, W. A. Hunt, and R. A. Harris, J. Neurochem. **47**, 489 (1986).
[12] J. D. Ashwell, R. H. Schwartz, J. B. Mitchell, and A. Russo, J. Immunol. **136**, 3649 (1986).
[13] G. J. Koteles, Radiat. Environ. Biophys. **21**, 1 (1982).
[14] K. Takahashi and I. Kaneko, Int. J. Radiat. Biol. **49**, 979 (1986).
[15] P. Mouillier, D. Daveloose, M. Dubos, F. Leterrier, and J. Hoebeke, Biochem. Biophys. Acta **883**, 407 (1986).
[16] A. Bonincontro, C. Cametti, A. Rosi, and L. Sportelli, Int. J. Radiat. Biol. **52**, 447 (1987).
[17] A. Canatafora, M. Ceccarini, L. Guidoni, F. Ianzini, M. Minetti, V. Viti, Int. J. Radiat. Biol. **51**, 59 (1987).
[18] N. Joshi, C. E. Swenberg, and M. J. McCreery, 7th Int. Rad. Res. Congress, Amsterdam, Book of Abstracts, 1982, p. b-15.
[19] B. R. Lentz, Chem. Phys. Lipids **50**, 171 (1989).
[20] R. M. Fiorini, M. Valentino, S. Wang, M. Glaser, and E. Gratton, Biochemistry **26**, 386 (1987).
[21] T. Parasassi, F. Conti, E. Gratton, and O. Sapora, Biochem. Biophys. Acta **898**, 196 (1987).
[22] T. Parasassi and E. Gratton, *Membrane Technology*, edited by R. Verna (Serono Symposia Publications, Raven, New York, 1979), Vol. 64, pp. 110–117.
[23] R. M. Fiorini, M. Valentino, M. Glaser, E. Gratton, and G. Curatola, Biochem. Biophys. Acta **939**, 485 (1988).
[24] M. Valentino, M. Governa, E. Gratton, R. M. Fiorini, G. Curatola, and E. Bertoli, FEBS Lett. **234**, 451 (1988).
[25] J. M. Beechem and E. Gratton, Proc. Soc. Photo-Opt. Instrum. Eng. **909**, 70 (1988).
[26] T. Parasassi, F. Conti, M. Glaser, and E. Gratton, J. Biol. Chem. **22**, 14,011 (1984).
[27] W. Leiko and G. Bartosz, Int. J. Radiat. Biol. **49**, 743 (1986).
[28] T. Nakazawa, K. Terayama, H. Okuali, and O. Yukawa, Biochem. Biophys. Acta **769**, 323 (1984).